

UV–Vis Spectroscopic Determination of the Dissociation Constant of Dichromate from 160 to 400 °C

Jerzy B. Chlistunoff and Keith P. Johnston*

Department of Chemical Engineering, The University of Texas at Austin, Austin, Texas 78712

Received: October 22, 1997; In Final Form: January 20, 1998

On the basis of direct measurements by UV–vis spectroscopy, the dissociation constant of dichromate was found to decrease with temperature from 160 to 400 °C. For fixed Cr(VI) and KOH concentrations, the molal concentration of HCrO_4^- initially increases with temperature but decreases again in the vicinity of water's critical point, where the density decreases substantially. The decrease in HCrO_4^- at high temperature and low density may be attributed to $(\text{K}^+)(\text{CrO}_4^{2-})$ ion pairs, to a high degree of electrostriction about CrO_4^{2-} , which facilitates the reaction $\text{HCrO}_4^- + \text{OH}^- = \text{CrO}_4^{2-} + \text{H}_2\text{O}$, and to ion activity coefficients.

Introduction

The development of hydrothermal technology in recent years^{1–5} has stimulated scientific interest in the properties of supercritical water systems. Acid–base and other ionic equilibria have been of special interest because of their central role in hydrothermal reactions, phase behavior, and corrosion. One of the important ions in hydrothermal technology is hexavalent chromium. Insoluble Cr(III) oxide may be separated from high-level nuclear wastes by hydrothermal oxidation to Cr(VI), which becomes soluble.⁶ Also, oxidation of Cr_2O_3 ^{7–13} is a reason some stainless steels (e.g., SS 316) lose their corrosion resistance in oxidative hydrothermal environments.^{13–16} This oxidation reaction may be used for the extraction of Cr from minerals.¹⁷ In all the above cases, the evaluation of the acid–base equilibria of Cr(VI) is of crucial importance for understanding and controlling reaction and separation processes.

Various complementary techniques have been used to study ionic equilibria under hydrothermal conditions including direct conductivity measurements,^{18–22} electrochemical pH measurements,^{18,23,24} and UV–vis spectroscopy.^{25–29} However, in electrochemical pH measurements, it is challenging to develop accurate reference electrodes for direct pH measurements under hydrothermal conditions, especially above 325 °C.²⁴ UV–vis spectroscopy is limited to equilibria involving species containing appropriate chromophores.^{30,31} Recently, stable pH indicators have been developed for temperatures up to 400 °C.^{25–29} Hexavalent chromium appears to be an ideal candidate for direct spectrophotometric study without an indicator, since all the Cr(VI) species absorb light in the UV and visible regions.³² This method^{33–44} and others^{45–51} have been used to study acid–base equilibria of Cr(VI) at 20 °C or slightly elevated temperatures. However, the potentiometric study by Palmer and co-workers⁵⁰ is the only high-temperature study (to 175 °C) of Cr(VI) equilibria.

The goal of this study is to evaluate the acid–base equilibria of Cr(VI) at temperatures up to 420 °C, where significant changes in the properties of water and ion solvation occur. Experimental techniques were developed for rapid measurement, given the accelerated corrosion of sapphire in basic solutions. The Results section begins with a description of spectra at ambient temperature and then up to 320 °C, where the spectral features are relatively easy to interpret. Next, more complex

behavior is described from 320 to 420 °C. A wide range of concentrations of KOH and HClO_4 were utilized to manipulate the acid–base equilibria and to calibrate the absorbances of the pure components, H_2CrO_4 , HCrO_4^- , and CrO_4^{2-} . In the next section, we determine the dissociation constant of HCrO_4^- to CrO_4^{2-} and $(\text{K}^+)(\text{CrO}_4^{2-})$ ion pairs, assuming that chromic acid and dichromate are not present. After analyzing the results in terms of ion pairing and electrostriction (contraction of water about an ion), we will justify this assumption with a detailed study of the dissociation of chromic acid.

Experimental Section

Freshly deionized water (Barnsted Nanopure II, specific resistivity > 17 M Ω cm) was used to prepare all the solutions. A stock 0.581 M solution of KOH was prepared from >97 wt % KOH (EM Scientific). The KOH pellets were first washed on an all-glass Buchner funnel to remove any surface K_2CO_3 , which may have formed in the reaction with CO_2 present in the air, and then dissolved in water. The concentration of the KOH solution was determined by titration of a standard solution of potassium hydrogen phthalate ACS (Aldrich).⁵² A stock solution of potassium dichromate ACS (Fisher Scientific) was prepared by dissolving a sample of the predried (120 °C) $\text{K}_2\text{Cr}_2\text{O}_7$ in deionized water and diluting it to a known volume. Diluted solutions of perchloric acid were prepared from concentrated, 60% perchloric acid (Aldrich), and their concentrations were determined by titration with a standard KOH solution by using phenolphthalein as an indicator. A solution of chromic acid was prepared by dissolving a sample of chromium trioxide (Baker Analyzed Reagent) in water and diluting to a known volume. The concentration of H_2CrO_4 solution was determined spectrophotometrically after converting it to CrO_4^{2-} with excess KOH.

All spectra were obtained with an apparatus modified from an earlier version.⁵³ A titanium optical cell with an aperture of 5 mm and a path length of 1 cm was equipped with two sapphire windows (Swiss Jewel Company).⁵⁴ The pressure in the tubing connected to the cell was measured with a Heise 710A digital gauge at low temperature. The solutions first were purged with nitrogen for 30 min. The spectra were measured with a Cary 3E UV–vis spectrophotometer and corrected for the baseline of pure water at an identical temperature and pressure. When

alkaline solutions at temperatures close to or above the critical point of water were studied, corrosion of the sapphire windows led to a progressive growth in the baseline. In such cases two baselines were recorded, one before and one after the experiment. The actual baseline was a weighted combination of both baselines, such that the average absorbance in the range 592–600 nm was zero, i.e., where absorption of light due to Cr(VI) is negligible. The typical time to fully exchange feed solution in the system was about 5 min. During this time the temperature in the cell dropped substantially and had to be equilibrated for a few additional minutes. For strongly alkaline solutions, this time was sufficiently long to result in strong window corrosion and, in consequence, to a solution pH change. Therefore, after the temperature was restored, the cell was flushed additionally with 0.5–1 mL of the solution, after which the temperature was equilibrated for a time not exceeding 1 min. The majority of the spectra were measured at a scan rate 360 nm/min, except for strongly alkaline media at temperatures close to or above the critical point, where scan rates of 720 nm/min or, extremely rarely, 1440 nm/min were used.

Since the spectra are difficult to fit with a small number of Gaussian peaks and the peak wavelengths of the pure solutes shift with temperature and density, we chose to use integrated areas. The absorbance for the wavelength range 320–550 nm was integrated numerically using trapezoidal rule.

Results and Discussion

Cr(VI) Spectra at Ambient Temperature and Pressure.

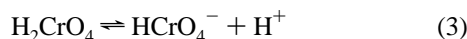
The principal equilibria in a Cr(VI) solution are⁵⁵



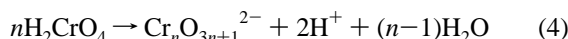
with $K_{12} = (3.4\text{--}5.0) \times 10^{14}$ at 25 °C,^{43,50}



with $K_{a2} = (2.82\text{--}3.16) \times 10^{-7}$ at 25 °C;^{39,50} and, in strongly acidic solutions,



with $K_{a1} = 1.5$ at 20 °C.^{55,56} Also, higher polychromates can be formed at high Cr(VI) concentrations in very strongly acidic media:⁴⁹



Similar condensation reactions occur between Cr(VI) and anions of other acids, e.g., HCl,^{37,38,50} H₂SO₄,³⁷ and H₃PO₄,⁵⁷ and species such as CrO₃Cl⁻, CrSO₇²⁻, and HCrPO₇²⁻ are formed.^{37,38,50,57}

All the Cr(VI) species listed above absorb light in the visible and ultraviolet regions due to charge-transfer transitions from orbitals localized mainly on the ligand atoms to an orbital localized mainly on Cr.³² Figure 1 shows the spectra of 2.50×10^{-4} M K₂Cr₂O₇ in different media. The spectra are rather similar for all the species listed above and exhibit two principal bands localized around 350–375 and 255–280 nm, which we call band I and II, respectively (Figure 1). Even though there are distinctive differences in band positions and molar absorptivities for the various Cr(VI) species, the bands are highly overlapped. Spectrum 1, obtained for a concentrated 5.82×10^{-2} M KOH solution, corresponds to CrO₄²⁻. Estimated concentrations of bichromate and dichromate in this solution are on the order of 10⁻¹⁰ and 10⁻¹⁸ M, respectively, based upon

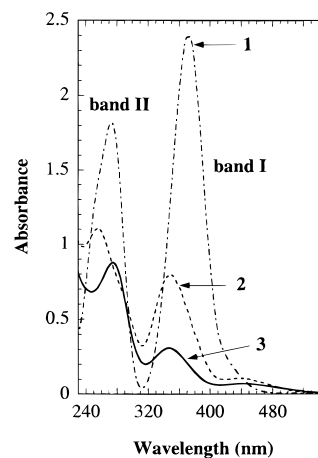


Figure 1. Ambient temperature and pressure spectra of 2.50×10^{-4} mol dm⁻³ K₂Cr₂O₇ solutions containing predominantly (see text) CrO₄²⁻ (curve 1, 5.82×10^{-2} mol dm⁻³ KOH); HCrO₄⁻ (curve 2, 9.2×10^{-3} mol dm⁻³ HClO₄); H₂CrO₄ (curve 3, 9.17 mol dm⁻³ HClO₄). Light path 1 cm.

the equilibrium constants listed above. The predominant species in the solution acidified with 9.2×10^{-3} M perchloric acid (spectrum 2) was HCrO₄⁻. The estimated contributions of chromic acid, dichromate, and chromate are less than 1.3%, 4.3%, and 0.005%, respectively. For spectrum 3 with concentrated 9.17 M perchloric acid, the predominant species is H₂CrO₄.^{55,56} Estimated contributions of dichromate and bichromate to the total Cr(VI) concentration are less than 8% and 39%, respectively. The spectra shown in Figure 1 agree well with the data published in the literature.^{33,34,36,42,58}

Cr(VI) Spectra up to 320 °C. Figure 2a shows the effect of temperature on the spectra of a 2.50×10^{-4} m K₂Cr₂O₇ solution containing a relatively small excess of KOH. These spectra were corrected for the density of the solution, which decreases with temperature. It was assumed that the solution density is equal to the density of water at the same temperature and pressure. The correction is made by dividing the measured absorbances by the density of water at a given temperature and pressure. At 20 °C the amounts of HCrO₄⁻, H₂CrO₄, and Cr₂O₇²⁻ are negligible, as discussed above, and the spectrum corresponds to the pure CrO₄²⁻ solution. A temperature increase leads to a gradual decrease of the two absorption bands and an increase in absorption at other wavelengths. At least three relatively well-defined isosbestic points are formed.

The observed spectral changes with temperature cannot be due to formation of the dichromate ion, since this reaction becomes progressively less favorable at elevated temperatures.⁵⁰ Also they are not caused by higher polychromates, which would require strongly acidic media and higher Cr(VI) concentrations.⁴⁹ The most likely explanation, based on both existing literature data⁵⁰ and theoretical predictions shown below, is that the temperature increase makes the dissociation of bichromate less favorable, leading to a progressive increase in HCrO₄⁻ and a corresponding decrease in the peak areas (see Figure 1). Indeed, the spectra recorded at higher temperatures (e.g., 320 °C, Figure 2b) resemble closely the spectra obtained for “pure” HCrO₄⁻ at room temperature (see Figure 1, curve 2), although slight shifts in wavelength are observed. The presence of the isosbestic points (Figure 2a) seems concordant with the suggested explanation of the spectral changes in terms of only two absorbing species, i.e., HCrO₄⁻ and CrO₄²⁻, remaining in chemical equilibrium. It cannot be regarded, however, as evidence for that for two reasons. First, these points are not true isosbestic points due to the temperature-driven changes in

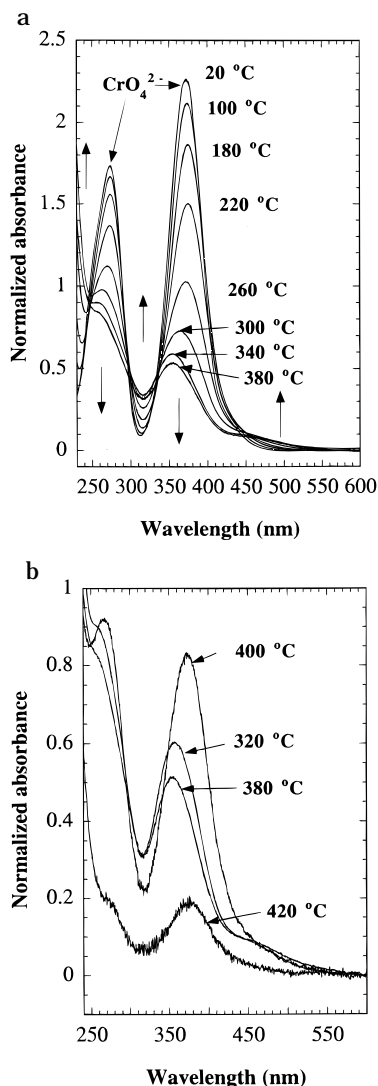


Figure 2. Temperature effect on the spectra of a 2.50×10^{-4} mol kg^{-1} $\text{K}_2\text{Cr}_2\text{O}_7$ solution with 1.98×10^{-3} mol kg^{-1} KOH at 27.6 MPa: (a) lower temperatures; (b) higher temperatures.

band shapes. Second, isosbestic points can also result in more complicated cases.^{59,60} Our estimates, based upon literature data for the $(\text{Na}^+)(\text{SO}_4^{2-})$ ⁶¹ ion pair, indicate that the $(\text{K}^+)(\text{CrO}_4^{2-})$ ion pair can contribute to the equilibrium at temperatures above 260 °C. To our knowledge the spectrum of the $(\text{K}^+)(\text{CrO}_4^{2-})$ ion pair has not been reported, but it is likely to be very similar to the spectrum of CrO_4^{2-} for two reasons. The spectra of aqueous CrO_4^{2-} resemble those of alkali metal chromates⁶² as well as our spectra at room temperature for 2.50×10^{-4} M $\text{K}_2\text{Cr}_2\text{O}_7 + 1.16 \times 10^{-2}$ M KOH solutions in water/dioxane mixtures. In the latter case the spectra recorded for pure aqueous solutions and mixtures containing up to 75% dioxane by volume, which have a significantly lower dielectric constant than water, were virtually identical. Unfortunately, higher concentrations of dioxane in the mixture could not be attained, because of either separation of the solution into water-rich and dioxane-rich phases or KOH/ K_2CrO_4 precipitation. Consequently, in addition to HCrO_4^- and CrO_4^{2-} , also the ion pair has to be considered in the analysis of the spectral data.

Cr(VI) Spectra from 320 to 420 °C. As shown in Figure 2, the spectra obtained in the temperature range 320–420 °C deviate from what can be expected on the basis of spectral changes observed at lower temperatures. For instance, an increase in temperature from 320 to 380 °C leads to a small

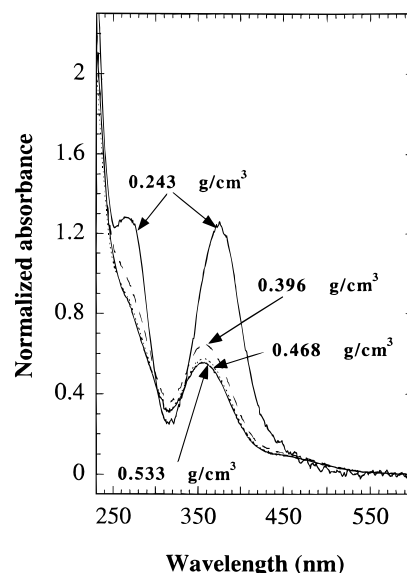


Figure 3. Effect of density on the spectra of Cr(VI) at 400 °C. $\text{K}_2\text{Cr}_2\text{O}_7$ concentration: 2.50×10^{-4} mol kg^{-1} . KOH concentration: 4.07×10^{-3} mol kg^{-1} .

decrease of absorbance at all the wavelengths for this slightly basic solution and the isosbestic points disappear (Figure 2a). Such a change may be due to a partial conversion of HCrO_4^- into chromic acid (see Figure 1), but a change in spectral parameters of bichromate cannot be ruled out.

A temperature increase from 380 to 400 °C seems to reverse the spectral changes that occurred at lower temperature. The measured area, corrected for water density, increases again and band I shifts back to longer wavelengths (Figure 2b). For instance, the spectra recorded for a 2.50×10^{-4} mol kg^{-1} $\text{K}_2\text{Cr}_2\text{O}_7 + 4.07 \times 10^{-3}$ mol kg^{-1} KOH solution at 400 and 260 °C were virtually identical. At higher densities (pressures) these effects are less prominent than at lower densities, as shown in Figure 3. A further temperature increase up to 420 °C at 27.6 MPa results in an abrupt decrease in the absorbance (Figure 2b), but the positions of band I and II, however, change very little. We will show that these changes are due to enhanced formation of ion pairs of CrO_4^{2-} and K^+ at temperatures higher than 380 °C and subsequent precipitation of K_2CrO_4 at 420 °C.

Similar effects of temperature on the area and position of band I are observed for a wide range in KOH concentration, as shown for 2.50×10^{-4} mol kg^{-1} $\text{K}_2\text{Cr}_2\text{O}_7$ solutions in Figures 4 and 5. As temperature increases, both the normalized area and wavelength maximum decrease up to 380 °C and then increase. In Figures 4 and 5, we have identified the properties of essentially pure CrO_4^{2-} and HCrO_4^- solutions with long arrows. The assignment of these arrows depends in part upon calculation of contributions to the measured band areas resulting from species other than bichromate and chromate, in particular dichromate and chromic acid. Since these calculations also rely in part on the two deprotonation equilibrium constants determined in this study, their results will be presented in the section dealing with error estimates. The band energy decreases (wavelength increases) with temperature for both species, and there is a slight decrease in the integrated area. Similarly, the energy of band II for pure HCrO_4^- and CrO_4^{2-} decreases (wavelength increases) with temperature. The magnitude of the solvatochromic effect for both charge-transfer bands is relatively small⁶³ because of small changes in actual electrical charge distribution in the chromate ion upon excitation.⁶⁴ Figure 5 provides additional evidence that the spectra of chromate and

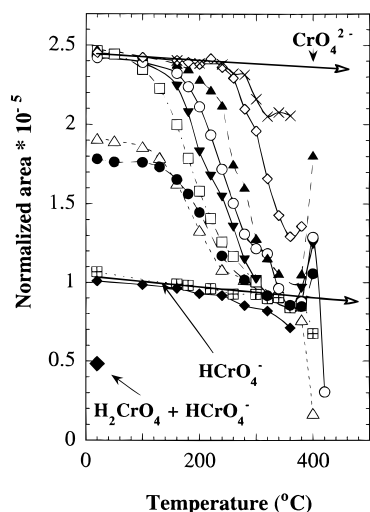


Figure 4. Temperature effect on the integrated area of band I normalized for density and Cr(VI) concentration for selected $\text{K}_2\text{Cr}_2\text{O}_7$ solutions at 27.6 MPa. The long arrows indicate the asymptotes characteristic for CrO_4^{2-} and HCrO_4^- (see text). $2.50 \times 10^{-4} \text{ mol kg}^{-1} \text{ K}_2\text{Cr}_2\text{O}_7$ with the following KOH concentrations (mol kg^{-1}): no KOH added (crossed square); 2.91×10^{-4} (Δ); 5.81×10^{-4} (\square); 9.88×10^{-4} (\blacktriangledown); 1.98×10^{-3} (\circ); 4.07×10^{-3} (\blacktriangle); 1.16×10^{-2} (\diamond); 5.81×10^{-2} (\times). Other solutions: $5.81 \times 10^{-3} \text{ mol kg}^{-1} \text{ KOH} + 5.00 \times 10^{-4} \text{ mol kg}^{-1} \text{ K}_2\text{Cr}_2\text{O}_7$ (\bullet); $2.50 \times 10^{-4} \text{ mol dm}^{-3} \text{ K}_2\text{Cr}_2\text{O}_7 + 3.83 \times 10^{-3} \text{ mol kg}^{-1} \text{ HClO}_4$ (\blacklozenge); $2.50 \times 10^{-4} \text{ mol dm}^{-3} \text{ K}_2\text{Cr}_2\text{O}_7 + 9.17 \text{ mol dm}^{-3} \text{ HClO}_4$ at ambient temperature and pressure (large \blacklozenge).

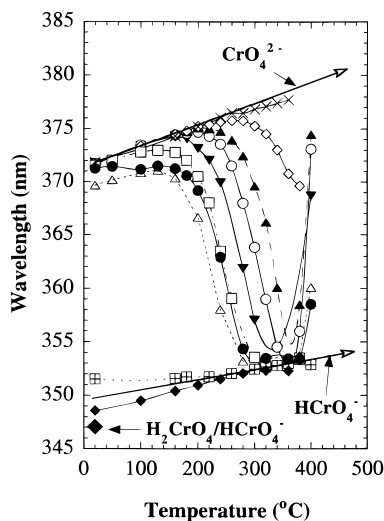


Figure 5. Temperature effect on the wavelength of band I for selected $\text{K}_2\text{Cr}_2\text{O}_7$ solutions at 27.6 MPa. The long arrows indicate the asymptotes characteristic for CrO_4^{2-} and HCrO_4^- (see text). For symbols as well as $\text{K}_2\text{Cr}_2\text{O}_7$, KOH, and HClO_4 concentrations refer to Figure 4.

the ion pair $(\text{K}^+)(\text{CrO}_4^{2-})$ are very similar. The wavelength of band I for chromate estimated at 360 °C is only around 1 nm longer than the wavelength measured in concentrated $5.81 \times 10^{-2} \text{ mol kg}^{-1} \text{ KOH}$ solution, in which the estimated⁶¹ ratio of the ion pair to chromate concentration is around 9:1.

A plot similar to Figure 5 is shown for band II in Figure 6. In this case, fewer solutions were characterized, because of the overlap of band II with a band in the far UV region (Figure 2b). The effect of protonation on band II is particularly important for the present study. While the wavelength of band I decreases from CrO_4^{2-} to HCrO_4^- to H_2CrO_4 , band II has similar energies for CrO_4^{2-} and H_2CrO_4 and significantly shorter wavelength for HCrO_4^- (see Figure 1). This large shift for HCrO_4^- makes it easier to decide which protonation equilibrium

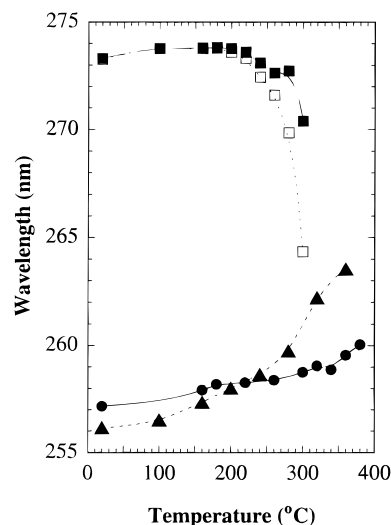


Figure 6. Temperature effect on the wavelength of band II for selected $2.50 \times 10^{-4} \text{ mol kg}^{-1} \text{ K}_2\text{Cr}_2\text{O}_7$ solutions at 27.6 MPa. KOH concentration (mol kg^{-1}): 6.97×10^{-3} (\blacksquare); 4.07×10^{-3} (\square); no additions (\bullet). HClO_4 concentration (mol kg^{-1}): 3.83×10^{-3} (\blacktriangle).

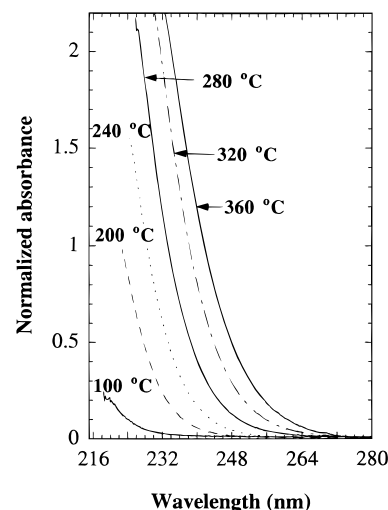


Figure 7. Spectra of $3.02 \times 10^{-3} \text{ mol kg}^{-1} \text{ KOH}$ at 27.6 MPa and different temperatures corrected for the absorption of pure water and solution density.

is predominant under experimental conditions and responsible for the observed spectral changes.

To determine if a charge transfer to solvent band for OH^- complicates our results, we measured spectra for a KOH solution without chromate (Figure 7). An examination of Figures 2 and 7 indicates that this band is at short enough wavelengths such that it does not interfere with the band I of Cr(VI).

Dissociation Constant of Bichromate, K_{a2} . In this section, we will assume that the only substances contributing to the measured absorbance are chromate, bichromate, and possibly the $(\text{K}^+)(\text{CrO}_4^{2-})$ ion pair in the entire temperature range for KOH concentrations above $5.81 \times 10^{-4} \text{ mol kg}^{-1}$. We will assume chromic acid and dichromate are not present. Because a large amount of detail will be required to justify this assumption, it will be presented in the last section of this study. We will also assume that the spectrum of the ion pair is identical to the CrO_4^{2-} spectrum. Based upon this assumption, the experimentally accessible quantities are bichromate concentration and the sum of the chromate and the ion pair concentrations. If this sum is replaced with an effective chromate concentration, an effective dissociation constant K_{a2}^{eff} may be defined.

The effective dissociation constant of bichromate may be determined spectroscopically, given the spectra of pure solutions of CrO_4^{2-} (in some cases with $(\text{K}^+)(\text{CrO}_4^{2-})$ ion pairs) and HCrO_4^- . By adding a sufficient excess of KOH, the concentration of HCrO_4^- is minimized, but corrosion of the sapphire windows can become a serious problem.²⁷ In addition, the density correction of the absorbance, which was based on the assumption of equal density for the solution and water, is less accurate at high KOH concentrations. However, for many of the alkaline solutions the integrated area of band I and its wavelength were found to be independent of the KOH concentration and close to corresponding parameters measured for CrO_4^{2-} at room temperature. These observations prove that bichromate is completely dissociated in the temperature range 20–220 °C (Figures 4 and 5) for the high KOH concentrations. In this temperature range there is also a negligible contribution from the $(\text{K}^+)(\text{CrO}_4^{2-})$ ion pair as estimated by assuming that the equilibrium constant for the ion pair is identical to that for $(\text{Na}^+)(\text{SO}_4^{2-})$.⁶¹ The areas of pure HCrO_4^- could not be obtained in a similar way, i.e., by measuring spectra of strongly acidified $\text{K}_2\text{Cr}_2\text{O}_7$ solutions. Unfortunately, dichromate, chromate, and chromic acid may be present along with HCrO_4^- . Therefore, a pure $\text{K}_2\text{Cr}_2\text{O}_7$ solution was used instead of acidified solutions. In this case an assumption was made that the areas measured for pure $2.50 \times 10^{-4} \text{ mol kg}^{-1} \text{ K}_2\text{Cr}_2\text{O}_7$ solutions in the temperature range 160–320 °C were equal to the areas characteristic for HCrO_4^- . In the next section, dealing with error estimates, this assumption will be shown to be valid.

It was also assumed that the integrated areas for pure CrO_4^{2-} and HCrO_4^- solutions at temperatures where they were not experimentally accessible can be obtained from extrapolations of the asymptotic lines, which were determined for pure chromate and bichromate (Figure 4). In addition, for pressures other than 27.6 MPa, for which less extensive studies were performed, it was assumed that the integrated areas for pure chromate and bichromate are identical to those measured at 27.6 MPa at a given temperature. This assumption is consistent with the small change in area in Figure 4 for HCrO_4^- over a wide temperature range, where density changed by a factor of 3.

By assuming that only bichromate, chromate, and the $(\text{K}^+)(\text{CrO}_4^{2-})$ ion pair are present in solution, K_{a2}^{eff} may be determined for a Cr(VI) solution as follows. The absorbance, A , at wavelength λ is given by:

$$A = \epsilon_\lambda [\text{Cr(VI)}]^0 = \epsilon_\lambda^{\text{HCrO}_4^-} [\text{HCrO}_4^-] + \epsilon_\lambda^{\text{CrO}_4^{2-}} [\text{CrO}_4^{2-}]^{\text{eff}} \quad (5)$$

where $[\text{Cr(VI)}]^0$ represents the initial molar concentration of Cr(VI) and ϵ_λ is the apparent molar extinction coefficient of the solution. Because of the change in water density with temperature and pressure, a standard state based upon molal concentrations is preferable.⁶⁵ For dilute electrolyte solutions, the molality of species S , m_s , may be obtained from the molarity as follows:

$$m_s = [S]/\rho \quad (6)$$

where ρ is the density of pure water. Substitution of eq 6 into eq 5 yields

$$A_{\text{norm}} = \epsilon_\lambda m_{\text{Cr(VI)}}^0 = \epsilon_\lambda 2m_{\text{K}_2\text{Cr}_2\text{O}_7}^0 = \epsilon_\lambda^{\text{HCrO}_4^-} m_{\text{HCrO}_4^-} + \epsilon_\lambda^{\text{CrO}_4^{2-}} m_{\text{CrO}_4^{2-}}^{\text{eff}} \quad (5a)$$

where $A_{\text{norm}} = A/\rho$.

Equation 5a can be integrated and combined with the Cr(VI) mass balance (shown below) to give

$$m_{\text{CrO}_4^{2-}}^{\text{eff}} = \left(\frac{E - E_{\text{HCrO}_4^-}}{E_{\text{CrO}_4^{2-}} - E_{\text{HCrO}_4^-}} \right) 2m_{\text{K}_2\text{Cr}_2\text{O}_7}^0 \quad (7)$$

$$m_{\text{HCrO}_4^-} = \left(\frac{E - E_{\text{CrO}_4^{2-}}}{E_{\text{HCrO}_4^-} - E_{\text{CrO}_4^{2-}}} \right) 2m_{\text{K}_2\text{Cr}_2\text{O}_7}^0 \quad (8)$$

where E , $E_{\text{HCrO}_4^-}$, and $E_{\text{CrO}_4^{2-}}$ correspond to the integrals in the range 320–550 nm of the measured extinction coefficients for the given solution, pure bichromate, and pure chromate, respectively.

An activity coefficient model is required to extract the desired equilibrium constants from the measured spectra. It is assumed that individual ionic activity coefficients are not sensitive to specific properties of ions, and for singly charged species they can be approximated by Pitzer's formula⁶⁶ for the mean ionic activity coefficient γ_\pm of a 1–1 electrolyte:

$$\ln \gamma_\pm = -A_\phi \left[\frac{I^{1/2}}{1 + bI^{1/2}} + \left(\frac{2}{b} \right) \ln(1 + bI^{1/2}) \right] \quad (9)$$

where $b = 1.2$. The ionic strength I is given by

$$I = (1/2) \sum_i m_i z_i^2 \quad (10)$$

where m_i and z_i are molalities and charges of all the ionic species in solution. The Debye–Huckel parameter A_ϕ is given by

$$A_\phi = (2\pi N_0 \rho / 1000)^{1/2} (e^2 / \epsilon \kappa T)^{3/2} / 3 \quad (11)$$

where N_0 is the Avogadro's number, e is the charge of the electron, ϵ is the dielectric constant of water as calculated by Uematsu and Franck,⁶⁷ and ρ is the water density calculated according to steam tables.⁶⁸ The activity coefficients for multiply charged ions are given by the formula^{69,70}

$$\ln \gamma_z = z^2 \ln \gamma_\pm \quad (12)$$

From the above assumptions, the Cr(VI) and K mass balances and the charge balance are given by

$$m_{\text{HCrO}_4^-} + m_{\text{CrO}_4^{2-}}^{\text{eff}} = 2m_{\text{K}_2\text{Cr}_2\text{O}_7}^0 \quad (13)$$

$$m_{\text{K}^+} + m_{\text{KOH}} = 2m_{\text{K}_2\text{Cr}_2\text{O}_7}^0 + m_{\text{KOH}}^0 \quad (14)$$

$$m_{\text{K}^+} + m_{\text{H}^+} = m_{\text{OH}^-} + m_{\text{HCrO}_4^-} + 2m_{\text{CrO}_4^{2-}}^{\text{eff}} \quad (15)$$

An effective dissociation constant for bichromate may be defined by

$$K_{a2}^{\text{eff}} = \frac{m_{\text{CrO}_4^{2-}}^{\text{eff}} m_{\text{H}^+} \gamma_\pm^4}{m_{\text{HCrO}_4^-}} \quad (16)$$

where the effective CrO_4^{2-} concentration includes ion pairs if present. The presence of ion pairs introduces some uncertainty into eqs 14 and 15, as discussed below. The equilibrium constant for KOH association¹⁹ is given by

$$K_{\text{as}} = \frac{m_{\text{KOH}}}{m_{\text{K}^+} m_{\text{OH}^-} \gamma_{\pm}^2} \quad (17)$$

and for the ionic product of water K_{w}^{71}

$$K_{\text{w}} = m_{\text{OH}^-} m_{\text{H}^+} \gamma_{\pm}^2 \quad (18)$$

All the concentrations and $K_{\text{a}2}^{\text{eff}}$ were calculated numerically by using an iterative procedure based on successive substitutions. An initial assumption was that all the ionic activity coefficients were equal to unity. Iterations were performed until variations in the mass and charge balances were lower than 1×10^{-15} mol kg⁻¹ and the variations in the equilibrium constants were on the order of 10⁻¹⁰% or less.

For the majority of temperatures, $K_{\text{a}2}^{\text{eff}}$ values at 27.6 MPa were obtained from measurements performed for 2.50×10^{-4} m K₂Cr₂O₇ solutions at six to eight different KOH concentrations. Some of the results were also obtained for 5.00×10^{-4} and 1.00×10^{-3} m K₂Cr₂O₇ solutions. Typical experimental results obtained for selected solutions and temperatures are given in Table 1. All of the measured equilibrium constants $K_{\text{a}2}^{\text{eff}}$ obtained are listed in Table 2, and Figure 8 shows the effect of temperature on $K_{\text{a}2}^{\text{eff}}$ at a constant pressure 27.6 MPa. In the temperature range 160–180 °C our data agree well with the data obtained from potentiometric measurements by Palmer and co-workers.⁵⁰ As is seen from Figure 8 the dissociation of bichromate (eq 2) is exothermic at 27.6 MPa, as expected for the reaction of a relatively strong acid. Part of the change in $K_{\text{a}2}^{\text{eff}}$ results from an isobaric decrease in density with temperature. The effect of density on $K_{\text{a}2}^{\text{eff}}$ at selected temperatures is shown in Figure 9. This ionogenic reaction, eq 2, is less favorable in low-density media, where the loss in the dielectric constant of water⁶⁷ decreases the ability of water to solvate ions.

The monotonic decrease of the bichromate dissociation constant with temperature may seem surprising, given the decrease in HCrO₄⁻ concentration at 400 °C. Two factors that influence this result will be considered. The first is the formation of ion pairs in the supercritical region due to the very low values of the dielectric constant. Also, the precipitation that occurs at 420 °C seems likely to be preceded by some aggregation in the solution phase. The second is the electrostriction of water about divalent CrO₄²⁻ versus that about monovalent ions.

An actual ratio of equilibrium molalities of the ion pair (K⁺)(CrO₄²⁻) and chromate ion is given by the formula

$$m_{\text{KCrO}_4^-} / m_{\text{CrO}_4^{2-}} = K_{\text{ip}} m_{\text{K}^+} \gamma_{\pm}^4 \quad (19)$$

Since K_{ip} is unknown, we assume that K_{ip} may be approximated by the equilibrium constant for (Na⁺)(SO₄²⁻) ion pair formation, which has been determined at pressures slightly above the vapor pressure up to 320 °C.⁶¹ Since neither m_{K^+} nor γ_{\pm} change significantly as a result of the ion pair formation in the solutions with low Cr(VI) concentration, the calculation of the concentration ratio given by eq 19 becomes much simpler. In this case, it is reasonable to use the K⁺ molalities and activity coefficients determined in the calculations of $K_{\text{a}2}^{\text{eff}}$ (eqs 13–18, Table 1). The above concentration ratio approaches 0.025 at 160 °C, 0.15 at 220 °C, 1.10 at 280 °C, and 3.25 at 320 °C for the highest initial KOH molalities applied, which were 3.02×10^{-3} , 6.97×10^{-3} , 1.74×10^{-2} , and 1.74×10^{-2} , respectively. These numbers are probably a little overestimated, since the larger K⁺ most likely forms weaker ion pairs than Na⁺.

An error in $K_{\text{a}2}$, generated by association of K⁺ and CrO₄²⁻, can be estimated, if it is assumed that the spectra of CrO₄²⁻ and (K⁺)(CrO₄²⁻) are identical, i.e., integrated areas for both species are equal as assumed above. In such a case the sum of CrO₄²⁻ and (K⁺)(CrO₄²⁻) molalities is determined from the measured spectra (eqs 5, 5a, 7). The effective equilibrium constant $K_{\text{a}2}^{\text{eff}}$ is then given by the equation

$$K_{\text{a}2}^{\text{eff}} = K_{\text{a}2}(1 + K_{\text{ip}} m_{\text{K}^+} \gamma_{\pm}^4) \quad (20)$$

The differences $\Delta pK_{\text{a}2}$ between negative logarithms of the estimated true ($K_{\text{a}2}$) and experimental, i.e., effective ($K_{\text{a}2}^{\text{eff}}$), dissociation constants may be obtained from this equation. The results, which were obtained for solutions in which the ratio of the HCrO₄⁻ concentration and effective CrO₄²⁻ concentration was closest to unity, are listed in Table 2 for the temperature range 160–360 °C. Similar estimates at temperatures higher than the critical temperature (374 °C) were not made due to the large error involved in extrapolation of the association constants for (Na⁺)(SO₄²⁻), which were determined along the saturation curve. At supercritical conditions, density would have a pronounced effect on ion pairing. Inspection of these data reveals that the effect of ion pairing on $K_{\text{a}2}$ remains within experimental error up to approximately 260 °C or perhaps up to a little higher temperature due to the possible overestimation of the ion pairing effect. At higher temperatures, modest differences are observed. Because (K⁺)(CrO₄²⁻) ion pairs are more stable than CrO₄²⁻ for low values of the dielectric constant, they play a major role in the increase in absorbance at 400 °C. The values of $K_{\text{a}2}^{\text{eff}}$ in Table 1 at a given temperature are relatively constant for a range in KOH concentration, suggesting that the term in parentheses in eq 20 is relatively constant. Either K_{ip} is sufficiently small or an increase in K⁺ is compensated by a decrease in γ_{\pm} . Because $K_{\text{a}2}$ is constant, it is of practical use in the determination of Cr(VI) equilibrium.

We now discuss the effect of electrostriction on the absorbance increase at 400 °C. Instead of examining the dissociation of bichromate ($K_{\text{a}2}$), it is more useful to consider the following isocoulombic reaction



This reaction is simply the difference between the dissociation of bichromate and water.

The equilibrium constant K_{bHA} for eq 21 is given by

$$K_{\text{bHA}} = K_{\text{a}2} / K_{\text{w}} \quad (22)$$

For the purpose of the following analysis it was assumed that $K_{\text{a}2}^{\text{eff}}$ was equal to $K_{\text{a}2}$.

A plot of log K_{bHA} versus $1/T$ (Figure 10) exhibits a minimum at 380 °C, and its increase at 400 °C seems to be in agreement with the observed decrease in the HCrO₄⁻ concentration. The data were fit by using a modified Born model^{26–29} as follows:

$$\ln K_{\text{bHA}}(T, \rho) = \ln K_{\text{bHA}}(T_0, \rho_0) + \left(\frac{\partial \ln K_{\text{bHA}}}{\partial (1/T)} \right)_{\rho_0} \left(\frac{1}{T} - \frac{1}{T_0} \right) - \frac{83459}{T} \left(\frac{1}{\epsilon(T, \rho)} - \frac{1}{\epsilon(T, \rho_0)} \right) \left(\frac{z_{\text{CrO}_4^{2-}}^2}{r_{\text{CrO}_4^{2-}}} - \frac{z_{\text{HCrO}_4^-}^2}{r_{\text{HCrO}_4^-}} - \frac{z_{\text{OH}^-}^2}{r_{\text{OH}^-}} \right) \quad (23)$$

where T_0 and ρ_0 are the reference temperature and density and z and r are charges and radii (in angstroms) of the various ions.

TABLE 1: Selected Experimental Data for 5.0×10^{-4} M Cr(IV) Solutions^a

area ^b	$m_{\text{KOH}}^0 \times 10^3$	$m_{\text{HCrO}_4^-} \times 10^4$	$m_{\text{CrO}_4^{2-}} \times 10^4$	$-\log m_{\text{H}^+}$	$I \times 10^3$	γ_{\pm}	$\text{p}K_{\text{a}2}$
		$t = 160 \text{ }^\circ\text{C}, p = 27.6 \text{ MPa}, d = 0.923 \text{ g cm}^{-3}, \text{p}K_{\text{w}} = 11.43$					
81.56	0.291	2.70	2.30	7.17	1.02	0.951	7.32
99.94	0.581	1.37	3.63	7.72	1.44	0.943	7.40
112.1	0.988	0.495	4.51	8.10	1.94	0.934	7.26
		$t = 240 \text{ }^\circ\text{C}, p = 27.6 \text{ MPa}, d = 0.837 \text{ g cm}^{-3}, \text{p}K_{\text{w}} = 11.01$					
85.96	1.975	2.23	2.77	8.15	2.74	0.902	8.23
		$t = 300 \text{ }^\circ\text{C}, p = 27.6 \text{ MPa}, d = 0.747 \text{ g cm}^{-3}, \text{p}K_{\text{w}} = 11.11$					
60.89	1.975	3.93	1.07	8.26	2.54	0.881	9.04
79.39	6.972	2.60	2.40	8.73	7.33	0.811	9.13
		$t = 360 \text{ }^\circ\text{C}, p = 27.6 \text{ MPa}, d = 0.604 \text{ g cm}^{-3}, \text{p}K_{\text{w}} = 11.91$					
49.81	3.02	4.61	0.390	9.16	3.33	0.804	10.62
64.70	11.6	3.54	1.46	9.57	10.4	0.688	10.61
		$t = 380 \text{ }^\circ\text{C}, p = 27.6 \text{ MPa}, d = 0.506 \text{ g cm}^{-3}, \text{p}K_{\text{w}} = 12.83$					
52.85	4.07	4.35	0.646	10.07	3.98	0.720	11.47
67.99	11.6	3.27	1.73	10.34	9.46	0.610	11.47
74.69	17.4	2.79	2.21	10.42	13.3	0.560	11.53
		$t = 400 \text{ }^\circ\text{C}, p = 27.6 \text{ MPa}, d = 0.243 \text{ g cm}^{-3}, \text{p}K_{\text{w}} = 17.15$					
62.32	0.988	3.64	1.36	13.29	1.23	0.547	14.76
64.44	1.975	3.49	1.51	13.50	1.72	0.492	15.09
90.51	4.07	1.62	3.38	13.60	2.98	0.397	14.89
105.7 ^c	0.581	8.63	1.37	12.94	1.50	0.515	14.89
		$t = 400 \text{ }^\circ\text{C}, p = 31.0 \text{ MPa}, d = 0.396 \text{ g cm}^{-3}, \text{p}K_{\text{w}} = 14.18$					
86.50	17.4	1.91	3.09	11.47	11.2	0.437	12.70
		$t = 400 \text{ }^\circ\text{C}, p = 34.5 \text{ MPa}, d = 0.468 \text{ g cm}^{-3}, \text{p}K_{\text{w}} = 13.17$					
77.73	17.4	2.53	2.47	10.66	12.2	0.527	11.78
		$t = 400 \text{ }^\circ\text{C}, p = 41.3 \text{ MPa}, d = 0.533 \text{ g cm}^{-3}, \text{p}K_{\text{w}} = 12.37$					
67.07	17.4	3.30	1.70	10.00	13.0	0.593	11.20

^a All the concentrations and ionic strengths expressed in molal concentration scale. The densities calculated according to ref 68. ^b A is the actual area integrated between 320 and 550 nm corrected for density. ^c $m_{\text{Cr(IV)}}^0 = 1.0 \times 10^{-3}$ mol kg⁻¹.

TABLE 2: Dissociation Constants of Bichromate ($K_{\text{a}2}$) and Chromic Acid ($K_{\text{a}1}$)

temperature (°C)	pressure (MPa)	density ^a (g cm ⁻³)	$\text{p}K_{\text{a}2}^{\text{eff } b}$	$\Delta \text{p}K_{\text{a}2}^c$	$\text{p}K_{\text{a}1}$
160	27.6	0.923	7.41 ± 0.11	0.004	
180		0.904	7.63 ± 0.11	0.006	
200		0.883	7.85 ± 0.07	0.009	1.70
220		0.861	8.00 ± 0.08	0.02	
240		0.837	8.17 ± 0.16	0.04	1.76
260		0.810	8.45 ± 0.06	0.09	
280		0.780	8.76 ± 0.07	0.17	2.02
300		0.747	9.13 ± 0.13	0.34	
320		0.709	9.49 ± 0.09	0.58	
340		0.663	9.94 ± 0.11	0.78	2.96
360		0.604	10.61 ± 0.11	0.95	
380		0.506	11.56 ± 0.03		
400		0.243	14.96 ± 0.14		
160	31.0	0.925	7.31		
200		0.885	7.80		
280		0.785	8.56		
400		0.396	12.70		
160	34.5	0.926	7.27		
200		0.888	7.80		
280		0.788	8.55		
400		0.468	11.78		
160	41.3	0.930	7.21		
200		0.892	7.74		
280		0.796	8.46		
400		0.533	11.20		

^a Ref 68. ^b The uncertainties in the $\text{p}K_{\text{a}2}^{\text{eff}}$ values determined at 27.6 MPa indicate one standard deviation. Because of fewer data points at other pressures, the statistical analysis could not be performed. ^c Estimated error in $\text{p}K_{\text{a}2}$ resulting from the $(\text{K}^+)(\text{CrO}_4^{2-})$ ion pair formation as described in the text.

In this model, the Born radii are adjusted from the bare ion values to include waters of hydration.

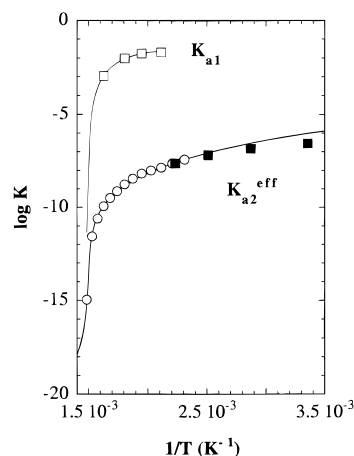


Figure 8. Effect of temperature on the dissociation constants of bichromate ($K_{\text{a}2}$) and chromic acid ($K_{\text{a}1}$) at constant pressure, 27.6 MPa. Solid squares: data taken from ref 50. Solid lines: calculated using modified Born equation (see text).

As in a previous study,²⁶ we assumed that the radius of the strongly hydrated OH^- ion equals 2.58 \AA^{72} and that the change of the Gibbs free energy of water with density is much smaller than the corresponding changes of the solvation energies of the ionic substances. The temperature 180 °C was selected as the reference temperature and the corresponding density (0.904 g cm^{-3}) as the reference density. The value of $(\partial \ln K_{\text{bHA}}/\partial(1/T))_{\rho_0}$ was 8543 K^{-1} and $\ln K_{\text{bHA}}(T_0, \rho_0)$ was 8.388. The equilibrium constants were underestimated over the entire temperature range when the radii of both chromate and bichromate were assumed equal to 1.646 \AA , i.e., the crystallographic radius of CrO_4^{2-} .³² Much better fits were obtained if a larger radius for the divalent and presumably strongly

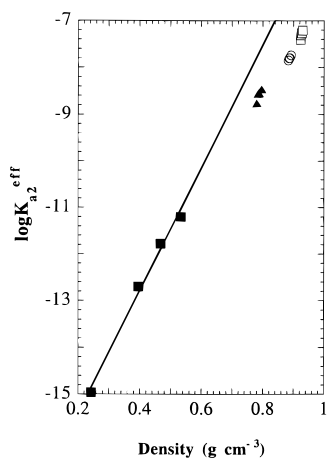


Figure 9. Effect of density on the dissociation constant of bichromate. Temperatures: 160 °C (□); 200 °C (○); 280 °C (▲); 400 °C (■).

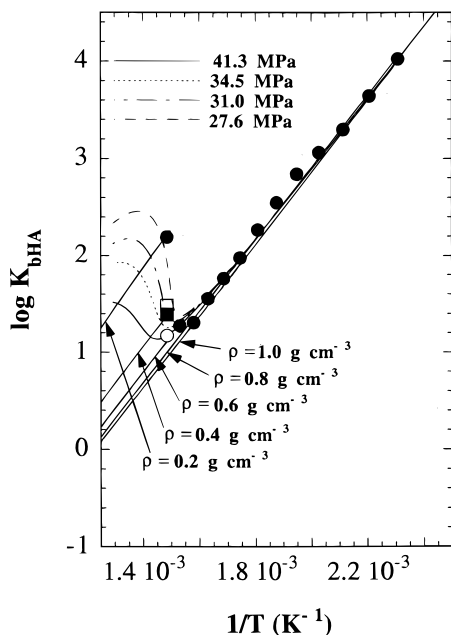


Figure 10. Effect of temperature and density on the equilibrium constant of the reaction $\text{HCrO}_4^- + \text{OH}^- \rightleftharpoons \text{CrO}_4^{2-} + \text{H}_2\text{O}$. Lines represent isobars and isochores calculated using the modified Born equation (see text). Experimental points obtained at the following pressures: 27.6 MPa (●); 31.0 MPa (□); 34.5 MPa (■); 41.3 MPa (○).

solvated CrO_4^{2-} was assumed, while keeping 1.646 Å for the radius of the singly charged HCrO_4^- . A value of 4.35 Å for the chromate ion radius resulted in the best fit (see Figure 10). The K_{bHA} values obtained at pressures higher than 27.6 MPa were also fitted well by eq 23 with the same radius (Figure 10).

A significant drop in the dielectric constant, which occurs in the temperature range 380–400 °C, leads to decreased solvation of all the ions. Since the Born solvation energy of an ion is proportional to z^2/r , the chromate ion would be strongly destabilized relative to the monovalent ions if it had a similar Born radius. The large radius regressed for CrO_4^{2-} may suggest that it is very strongly hydrated and may probably retain its first two coordination shells even in supercritical water. This hypothesis is supported by radial distribution functions for divalent cations.⁷³ However, the unusually large effective radius may indirectly reflect the ion pairing of CrO_4^{2-} relative to HCrO_4^- in low ϵ media.

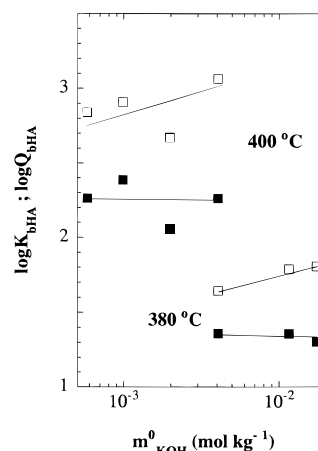


Figure 11. Equilibrium constants (open symbols) for the reaction of bichromate with OH^- and corresponding concentration quotients (filled symbols) at 27.6 MPa and selected temperatures.

Strong ion–ion interactions in solutions with low dielectric constant lead not only to ionic association but also to lowering of ionic activity coefficients (Table 1). Even though the boundary between these two phenomena is somewhat arbitrary, they may be discussed separately with generally accepted models. Figure 11 shows the experimental values of the equilibrium constant K_{bHA} and the corresponding equilibrium quotient Q_{bHA} . The Q_{bHA} was determined from eq 16 with $\gamma_{\pm} = 1$. As can be seen, $\log Q_{\text{bHA}}$ measured at 400 °C for $4.067 \times 10^{-3} \text{ mol kg}^{-1}$ KOH is approximately 0.8 log units higher than $\log K_{\text{bHA}}$, whereas the difference measured at 380 °C is only around 0.3 log units, even though the ionic strength in the latter case was higher. In other words, low activity coefficients shift the equilibrium toward formation of CrO_4^{2-} , in a similar way as solubility of a sparingly soluble salt increases in the presence of high ionic strengths of an indifferent electrolyte. The effect is especially strong at 400 °C and can contribute also to the observed increase in absorbance at this temperature.

Verification of the Assumptions and Error Estimates. It can be expected that the principal source of error in the present work is the neglect of the species other than chromate and bichromate in the Cr(VI) equilibria. The integrated areas used for calibration of the pure chromate and bichromate ions (eqs 7 and 8) can be distorted by the presence of these other species. These other species will also produce errors in application of eq 5a. An accurate estimate of these errors is possible only when all the equilibrium constants and integrated areas for all the species considered are known, which is not possible in the present study. However, a detailed analysis of the results, presented below, suggests that the equilibrium constants presented above are reasonably accurate.

(i) Errors in the Integrated Areas for Standard Chromate and Bichromate Standard Solutions. The accuracy of the determination of the integrated areas for the HCrO_4^- and CrO_4^{2-} standards can be estimated by using the values of K_{a2} determined in this study as well as estimated equilibrium constants for the formation of dichromate and chromic acid. The standard solutions are used to determine $E_{\text{HCrO}_4^-}$ and $E_{\text{CrO}_4^{2-}}$ in eqs 7–8. The equilibrium constant K_{21} for dichromate formation (eq 1) in the range 25–175 °C can be calculated from the data of Palmer et al.,⁵⁰ whereas for higher temperatures, they can be obtained from extrapolation of the linear dependence of $\log K_{21}$ versus the inverse temperature. The dissociation constants K_{a1} of chromic acid (eq 2) were estimated from our own experiments, as described in the next section.

Pure $K_2Cr_2O_7$ solutions were used as standard $HCrO_4^-$ solutions in the temperature range 160–320 °C. To determine the contribution of dichromate to the Cr(VI) mass balance, eqs 9–12 and modified equations for mass and charge balances to include $Cr_2O_7^{2-}$ were used. In addition, an expression for the equilibrium constant of reaction 1 was included:

$$K_{21} = \frac{m_{Cr_2O_7^{2-}}}{m_{CrO_4^{2-}} m_{H^+}^2 \gamma_{\pm}^2} \quad (24)$$

At 160 °C, the calculated molalities of $HCrO_4^-$, CrO_4^{2-} , and $Cr_2O_7^{2-}$ were 4.9×10^{-4} , 4.3×10^{-6} , and 1.5×10^{-6} mol kg^{-1} , respectively. At 320 °C they were 5.0×10^{-4} , 8.2×10^{-8} , and 5.0×10^{-7} mol kg^{-1} , respectively. In both cases, the concentration of both impurities is negligible compared with bichromate.

The integrated area for the dichromate ion³⁴ is about 1.5 times the area measured for the identical Cr(VI) equivalents of $HCrO_4^-$. The integrated area for chromate, on the other hand, is roughly 2.4 times larger than the area for $HCrO_4^-$. The estimated error of the integrated bichromate area measured for a 2.50×10^{-4} mol kg^{-1} $K_2Cr_2O_7$ solution from the presence of dichromate and chromate can be estimated as 1.6% at 160 °C and 0.14% at 320 °C. This negligible contribution is even smaller at higher temperatures.

The contribution of chromic acid to the absorbance of $K_2Cr_2O_7$ solutions, which were used as $HCrO_4^-$ standards, was estimated in the temperature range 200–340 °C, for which K_{a1} was determined as shown in the next section. Only monomeric Cr(VI) species were considered in the mass balance. At 200 °C the calculated concentrations of $HCrO_4^-$, CrO_4^{2-} , and H_2CrO_4 were 5.0×10^{-4} , 2.1×10^{-6} , and 9.1×10^{-8} mol kg^{-1} , respectively. At 340 °C the calculated concentrations were 5.0×10^{-4} , 4.7×10^{-8} , and 6.5×10^{-7} mol kg^{-1} , respectively. Since concentrations of both H_2CrO_4 and CrO_4^{2-} are at least 2 orders of magnitude lower than $HCrO_4^-$ concentration, their contribution to the measured absorbance of pure $K_2Cr_2O_7$ solutions is negligible in the temperature range 200–340 °C. The contribution resulting from the presence of H_2CrO_4 should be even smaller at 160 °C. In conclusion, pure 2.50×10^{-4} mol kg^{-1} $K_2Cr_2O_7$ solutions contain almost exclusively $HCrO_4^-$ in the temperature range 160–340 °C and can be used as standard $HCrO_4^-$ solutions for the spectrophotometric determination of the Cr(VI) acid–base equilibrium constants.

(ii) Estimate of the Dissociation Constant K_{a1} of Chromic Acid. There are no published data on the dissociation of chromic acid at high temperatures, and extrapolation from the limited data at temperatures close to 20 °C^{33,37,56} would be very inaccurate. Our approximate determination of K_{a1} was based on spectral measurements for $K_2Cr_2O_7$ and H_2CrO_4 solutions as well as $K_2Cr_2O_7$ solutions acidified with perchloric acid. Perchloric acid is believed³⁷ not to form substituted chromates. However, it slowly decomposes to chlorine and oxygen at elevated temperatures.⁷⁴ To test the stability of perchloric acid, we measured spectra of a 0.01 *m* $HClO_4$ solution in the temperature range 200–360 °C. We observed no decomposition of the acid for temperatures up to 300 °C and residence times as long as 30 min, which agrees with reported slow kinetics.⁷⁴ At 360 °C and for residence times longer than 10 min a weak band with an absorption maximum around 370 nm was detected. Since intermediates of the reaction are unstable,⁷⁴ the band was interpreted to be molecular chlorine, even though it was red shifted by some 40 nm from its position in the gas phase.⁷⁵ Approximately 6% of the acid decomposed after 0.5 h, giving

rise to a density-corrected absorbance on the order of 0.025. With the much shorter residence times employed in our experiments, typically around 2 min, decomposition of $HClO_4$ is not expected to influence the composition of a Cr(VI) solution nor its spectrum.

We found that the areas normalized for Cr(VI) concentration, measured for 5.70×10^{-4} *m* chromic acid, pure 2.50×10^{-4} *m* $K_2Cr_2O_7$, as well as 2.50×10^{-4} *m* $K_2Cr_2O_7$ acidified with 3.83×10^{-3} *m* or less concentrated $HClO_4$, were very similar in the temperature range 20–320 °C, indicating H_2CrO_4 was not formed in significant quantities. A large decrease in absorbance, most likely due to formation of chromic acid (see Figure 1), could be observed for 2.50×10^{-4} *m* $K_2Cr_2O_7$ solution acidified with 9.31×10^{-3} *m* $HClO_4$ in the temperature range 200–280 °C, 5.70×10^{-4} *m* H_2CrO_4 without $HClO_4$ at 340 °C, and 2.50×10^{-4} *m* $K_2Cr_2O_7$ acidified with 3.83×10^{-3} *m* $HClO_4$ at 360 °C. It was assumed that chromates and dichromates were not formed, which seemed reasonable in the light of calculations presented above. It was also assumed that perchloric acid was fully dissociated in this temperature range.⁷⁶

The actual concentration ratios of chromic acid and bichromate for the acidified solutions were calculated from integrated normalized absorbances by using equations analogous to eqs 7 and 8. Because of the lack of a more reasonable estimate, it was assumed that the normalized area for pure chromic acid is equal to the one measured at room temperature in 9.17 M perchloric acid. Since $HCrO_4^-$ is probably not completely protonated in this medium (see above), this area is most likely overestimated. An overestimate of the area for H_2CrO_4 is expected to result in an underestimated K_{a1} or an upper bound on the concentration of H_2CrO_4 . The area for pure bichromate was the one used for the determination of the K_{a2} . The Cr(VI) mass balance is

$$m_{HCrO_4^-} + m_{H_2CrO_4} + m_{CrO_4^{2-}} = 2m_{K_2Cr_2O_7}^0 \quad (13a)$$

for a dichromate feed solution and

$$m_{HCrO_4^-} + m_{H_2CrO_4} + m_{CrO_4^{2-}} = m_{H_2CrO_4}^0 \quad (13b)$$

for chromic acid feed solution. The potassium mass balance for a $K_2Cr_2O_7$ feed solution is

$$m_{K^+} = 2m_{K_2Cr_2O_7}^0 \quad (14a)$$

The charge balance for a $K_2Cr_2O_7$ feed solution is

$$m_{K^+} + m_{H^+} = m_{OH^-} + m_{HCrO_4^-} + m_{ClO_4^-} + 2m_{CrO_4^{2-}} \quad (15a)$$

or for a H_2CrO_4 solution is

$$m_{H^+} = m_{OH^-} + m_{HCrO_4^-} + 2m_{CrO_4^{2-}} \quad (15b)$$

The following expression was used for the equilibrium constant of reaction 3:

$$K_{a1} = (m_{HCrO_4^-} m_{H^+} \gamma_{\pm}^2) / m_{H_2CrO_4} \quad (25)$$

From K_{a1} , equilibrium constants for the isocoulombic reaction between H_2CrO_4 and OH^- were calculated and modeled with a modified Born equation^{26–29} similar to eq 23. The reference temperature was selected as 240 °C, and the radius of $HCrO_4^-$ was assumed to be equal to the crystallographic radius of CrO_4^{2-} , i.e., 1.646 Å.³² The model fit the equilibrium constants obtained in the temperature range 200–340 °C (Figure 8 and

Table 2). However, the equilibrium constant obtained from the experiment performed at 360 °C with the solution acidified with $3.83 \times 10^{-3} \text{ m HClO}_4$ deviated strongly from the model, indicating that perchloric acid was not fully dissociated under these conditions. The model was further used to calculate the dissociation constants of chromic acid at temperatures higher than 340 °C.

(iii) Errors in Density. The accuracy of the normalized absorbance depends on the uncertainty in the solution density. We have utilized density data for NaCl solutions to estimate the effect of solution density on $m_{\text{HCrO}_4^-}$. The density of a 0.2% NaCl (approximately $3.4 \times 10^{-2} \text{ mol kg}^{-1}$) solution at 396 °C and 271 atm pressure, i.e., under conditions very similar to our experiments, is around 7% higher than the pure steam density under identical conditions.⁷⁷ At lower temperatures this difference is smaller. Consequently, the absorbance measured at 400 °C and 27.6 MPa for our more dilute solutions may be overestimated by approximately 7%, whereas the observed increase in the normalized absorbance is much higher (Figure 4). In addition, the absorbance increase is accompanied by a spectral shift indicating a change in equilibrium, not just a change in $m_{\text{HCrO}_4^-}$ (Figures 4 and 5). Clearly, the density effect on the normalized absorbances is minor compared with the change in chemical equilibrium.

(iv) Other Sources of Error. A 1% uncertainty in KOH concentration produces an uncertainty of 0.1 in $\text{p}K_{a2}$ at 160 °C for the lowest KOH concentration ($2.91 \times 10^{-4} \text{ m}$) and 0.03 for the highest concentration. At 180 °C the corresponding numbers are 0.05 and 0.03, while for other temperatures they usually do not exceed 0.03. The uncertainty due to uncertainties in band areas strongly depends on the chromate/bichromate ratio and may be as high as 0.15 for a 2% uncertainty in the measured area at 160 °C, but it quickly drops to around 0.05 at higher temperatures.

Conclusions

Acid–base equilibria of Cr(VI) may be measured directly by UV–vis spectroscopy up to 400 °C. The deprotonation of the HCrO_4^- becomes less favorable as the temperature of alkaline solutions ($m_{\text{KOH}}^0 \geq 5.81 \times 10^{-4} \text{ mol kg}^{-1}$) of Cr(VI) is raised from 20 to 260 °C. Bichromate is a sufficiently strong acid such that deprotonation is exothermic. At higher temperatures, K_{a2} decreases faster than at lower temperatures due to an isobaric decrease in density. From 380 to 400 °C, the HCrO_4^- concentration decreases unlike the case at lower temperatures. Ion pair formation of $(\text{K}^+)(\text{CrO}_4^{2-})$ becomes very favorable even in weakly alkaline solutions. Also pronounced electrostriction of water about CrO_4^{2-} and nonspecific effects of activity coefficients (ionic strength) can contribute to the decreased stability of HCrO_4^- in the supercritical region. These effects are best understood by examining the relative acidity of bichromate versus water, described by the reaction $\text{HCrO}_4^- + \text{OH}^- = \text{CrO}_4^{2-} + \text{H}_2\text{O}$, rather than K_{a2} . Progressive ionic association eventually leads to K_2CrO_4 precipitation at 420 °C.

Acknowledgment. We gratefully acknowledge support from the Department of Energy (DE-FG07-96ER14687), from the U.S. Army for a University Research Initiative Grant (30374-CH-URI), from the R.A. Welch Foundation, and from the Separations Research Program at the University of Texas, a consortium of over 30 companies. We thank Steve Buelow and Kirk Ziegler for useful discussions.

References and Notes

(1) Tester, J. W.; Holgate, H. R.; Armellini, F. J.; Webley, P. A.; Killilea, W. R.; Hong, G. T.; Barner, H. E. In *ACS Symposium Series 518*.

- Emerging Technologies in Hazardous Waste Management*; Tedder, D. W., Pohland, F. G., Eds.; American Chemical Society: Washington, DC, 1993; pp 35–76.
- (2) Sealock, J.; Elliott, D. C.; Baker, E. G.; Butner, R. S. *Ind. Eng. Chem. Res.* **1993**, *32*, 1535.
- (3) Shaw, R. W.; Brill, T. B.; Clifford, A. A.; Eckert, C. A.; Franck, E. U. *Chem. Eng. News* **1991**, 26.
- (4) Gloyna, E. F.; Li, L. *Waste Manage.* **1993**, *13*, 379.
- (5) Savage, P. E.; Gopalan, S.; Mizan, T. I.; Martino, C. J.; Brock, E. E. *AIChE J.* **1995**, *41*, 1723.
- (6) Oldenborg, R.; Robinson, J. M.; Buelow, S. J.; Dyer, R. B.; Anderson, G.; Dell'Orco, P. C.; Funk, K.; Willmanns, E.; Knutsen, K. LA-UR-94:3233, Hydrothermal Processing of Inorganic Components of Hanford Tank Wastes, Los Alamos National Laboratories, 1994.
- (7) Valverde, N. *Ber. Bunsen-Ges.* **1976**, *80*, 333.
- (8) Segal, M. G.; Williams, W. J. *J. Chem. Soc., Faraday Trans. 1* **1986**, *82*, 3245.
- (9) O'Brien, A. B.; Segal, M. G.; Williams, W. J. *J. Chem. Soc., Faraday Trans. 1* **1987**, *83*, 371.
- (10) Rodenas, L. G.; Morando, P. J.; Blesa, M. A.; Duhalde, S.; Saragovi, C. *Can. J. Chem.* **1993**, *71*, 771.
- (11) Mills, A.; Sawunyama, P. *J. Chem. Soc., Faraday Trans.* **1993**, *89*, 3389.
- (12) Reartes, G. B.; Morando, P. J.; Blesa, M. A.; Hewlett, P. B.; Matijevic, E. *Langmuir* **1995**, *11*, 2277.
- (13) Aki, N. V. K. S.; Ding, Z.-Y.; Abraham, M. A. *AIChE J.* **1996**, *42*, 1995.
- (14) Huang, S.; Daehling, K.; Carleson, T. E.; Taylor, P.; Wai, C.; Propp, A. In *ACS Symposium Series 406. Supercritical Fluid Science and Technology*; Johnston, K. P., Penninger, J. M. L., Eds.; American Chemical Society: Washington, DC, 1989; pp 276–286.
- (15) Huang, S.; Daehling, K.; Carleson, T. E.; Abdel-Latif, M.; Taylor, P.; Wai, C.; Propp, A. In *ACS Symposium Series 406. Supercritical Fluid Science and Technology*; Johnston, K. P., Penninger, J. M. L., Eds.; American Chemical Society: Washington, DC, 1989; pp 287–300.
- (16) Rollans, S.; Gloyna, E. F. *Technical Report CRWR 240*, Center for Research in Water Resources: The University of Texas at Austin, 1993.
- (17) Yamasaki, N.; Kanahara, S.; Yanagisawa, K.; Matsuoka, K. *Nippon Kagaku Kaishi* **1982**, *12*, 1903.
- (18) Mesmer, R. E.; Marshall, W. L.; Palmer, D. A.; Simonson, J. M.; Holmes, H. F. *J. Solution Chem.* **1988**, *17*, 699.
- (19) Ho, P. C.; Palmer, D. A. In *Physical Chemistry of Aqueous Systems: Meeting the Needs of Industry. Proceedings of the 12th International Conference on the Properties of Water and Steam*; White, H. J., Jr., Sengers, J. V., Neumann, D. B., Bellows, J. C., Eds.; Begell House: New York, 1994; p 518.
- (20) Ho, P. C.; Palmer, D. A.; Mesmer, R. E. *J. Solution Chem.* **1994**, *23*, 997.
- (21) Zimmerman, G. H.; Gruszkiewicz, M. S.; Wood, R. H. *J. Phys. Chem.* **1995**, *99*, 11612.
- (22) Ho, P. C.; Palmer, D. A. *J. Solution Chem.* **1996**, *25*, 711.
- (23) Mesmer, R. E.; Holmes, H. F. *J. Solution Chem.* **1992**, *21*, 725.
- (24) Macdonald, D. D.; Hettiarachchi, S.; Song, H.; Makela, K.; Emerson, R.; Ben-Haim, M. *J. Solution Chem.* **1992**, *21*, 849.
- (25) Shin, T.-W.; Kim, K.; Lee, I.-J. *J. Solution Chem.* **1997**, *26*, 379.
- (26) Xiang, T.; Johnston, K. P. *J. Phys. Chem.* **1994**, *98*, 7915.
- (27) Xiang, T.; Johnston, K. P.; Wofford, W. T.; Gloyna, E. F. *Ind. Eng. Chem. Res.* **1996**, *35*, 4788.
- (28) Xiang, T.; Johnston, K. P. *J. Solution Chem.* **1997**, *26*, 13.
- (29) Ryan, E. T.; Xiang, T.; Johnston, K. P.; Fox, M. A. *J. Phys. Chem. A* **1997**, *101*, 1827.
- (30) Heinrich, C. A.; Seward, T. M. *Geochim. Cosmochim. Acta* **1990**, *54*, 2207.
- (31) Seward, T. M. *Geochim. Cosmochim. Acta* **1984**, *48*, 121.
- (32) Cieslak-Golonka, M. *Coord. Chem. Rev.* **1991**, *109*, 223.
- (33) Tong, J. Y.; King, E. L. *J. Am. Chem. Soc.* **1953**, *75*, 6180.
- (34) Davies, W. G.; Prue, J. E. *Trans. Faraday Soc.* **1955**, *51*, 1045.
- (35) Howard, J. R.; Nair, V. S. K.; Nancollas, G. H. *Trans. Faraday Soc.* **1958**, *54*, 1034.
- (36) Sasaki, Y. *Acta Chem. Scand.* **1962**, *16*, 719.
- (37) Haight, J. G. P.; Richardson, D. C.; Coburn, N. H. *Inorg. Chem.* **1964**, *3*, 1777.
- (38) Tong, J. Y.; Johnson, R. L. *Inorg. Chem.* **1966**, *5*, 1902.
- (39) Linge, H. G.; Jones, A. L. *Aust. J. Chem.* **1968**, *21*, 2189.
- (40) Perlmutter-Hayman, B.; Weissmann, Y. *Is. J. Chem.* **1968**, *6*, 17.
- (41) Grace, M. R.; Tregloan, P. A. *Polyhedron* **1992**, *11*, 2069.
- (42) Olazabal, M. A.; Borge, G.; Castano, R.; Etxebarria, N.; Madariaga, J. M. *J. Solution Chem.* **1993**, *22*, 825.
- (43) Linge, H. G.; Jones, A. L. *Aust. J. Chem.* **1968**, *21*, 1445.
- (44) Clare, B. W.; Druskovich, D. M.; Kepert, D. L.; Kyle, J. H. *Aust. J. Chem.* **1977**, *30*, 211.
- (45) Neuss, J. D.; Rieman, D. W., III. *J. Am. Chem. Soc.* **1934**, *56*, 2238.

- (46) Hepler, L. G. *J. Am. Chem. Soc.* **1958**, *80*, 6183.
(47) Jones, A. L.; Linge, H. G. *Aust. J. Chem.* **1969**, *22*, 663.
(48) Michel, G.; Machiroux, R. *J. Raman Spectrosc.* **1983**, *14*, 22.
(49) Michel, G.; Cahay, R. *J. Raman Spectrosc.* **1986**, *17*, 79.
(50) Palmer, D. A.; Wesolowski, D.; Mesmer, R. E. *J. Solution Chem.* **1987**, *16*, 443.
(51) Palmer, D. A.; Begun, G. M.; Ward, F. H. *Rev. Sci. Instrum.* **1993**, *64*, 1994.
(52) *Official Methods of Analysis of AOAC International*, 16th ed.; AOAC International: Arlington, 1995; Vol. II, p A.1.12.
(53) Bennett, G. E.; Johnston, K. P. *J. Phys. Chem.* **1994**, *98*, 441.
(54) Johnston, K. P.; Chlistunoff, J. B. *J. Supercritical Fluids*, in press.
(55) Baes, C. F., Jr.; Mesmer, R. E. *The Hydrolysis of Cations*; Wiley-Interscience: New York, 1976.
(56) Lukkari, O. *Suomen Kem.* **1970**, *43B*, 347.
(57) Holloway, F. *J. Am. Chem. Soc.* **1952**, *74*, 224.
(58) Brasch, N. E.; Buckingham, D. A.; Bram Evans, A.; Clark, C. R. *J. Am. Chem. Soc.* **1996**, *118*, 7969.
(59) Brynstad, J.; Smith, G. P. *J. Phys. Chem.* **1968**, *72*, 296.
(60) Nowicka-Jankowska, T. *J. Inorg. Nucl. Chem.* **1971**, *33*, 2043.
(61) Oscarson, J. L.; Izatt, R. M.; Brown, P. R.; Pawlak, Z.; Gillespie, S. E.; Christensen, J. J. *J. Solution Chem.* **1988**, *17*, 841.
(62) Johnson, L. W.; McGlynn, S. P. *Chem. Phys. Lett.* **1970**, *7*, 618.
(63) Liptay, W. *Angew. Chem., Int. Ed. Engl.* **1969**, *8*, 177.
(64) Miller, R. M.; Tinti, D. S.; Case, D. A. *Inorg. Chem.* **1989**, *28*, 2738.
(65) Chen, X.; Izatt, R. M.; Oscarson, J. L. *Chem. Rev.* **1994**, *94*, 467.
(66) Pitzer, K. S. In *Activity Coefficients in Electrolyte Solutions*, 2nd ed.; pp 75–153.
(67) Uematsu, M.; Franck, E. U. *J. Phys. Chem. Ref. Data* **1980**, *9*, 1291.
(68) Haar, L.; Gallagher, J. S.; Kell, G. S. *NBS/NRC Steam Tables*; Hemisphere: Washington, DC, 1984.
(69) Oscarson, J. L.; Gillespie, S. E.; Izatt, R. M.; Chen, X.; Pando, C. *J. Solution Chem.* **1992**, *21*, 789.
(70) Ziemniak, S. J. *J. Solution Chem.* **1995**, *24*, 837.
(71) Marshall, W. L.; Franck, E. U. *J. Phys. Chem. Ref. Data* **1981**, *10*, 1.
(72) Tanger, J. C., IV; Pitzer, K. S. *J. Phys. Chem.* **1989**, *93*, 4941.
(73) Flanagan, L. W.; Balbuena, P. B.; Johnston, K. P.; Rossky, P. J. *J. Phys. Chem.* **1997**, *101*, 7798.
(74) Henderson, M. P.; Miasek, V. I.; Swaddle, T. W. *Can. J. Chem.* **1971**, *49*, 317.
(75) Fergusson, W. C.; Slotin, L.; Style, D. W. *Trans. Faraday Soc.* **1936**, *32*, 956.
(76) Ratcliffe, C. I.; Irish, D. E. *Can. J. Chem.* **1984**, *62*, 1134.
(77) Benson, S. W.; Copeland, C. S.; Pearson, D. J. *Chem. Phys.* **1953**, *21*, 2208.